Atmos. Chem. Phys. Discuss., 14, 16691–16729, 2014
www.atmos-chem-phys-discuss.net/14/16691/2014/
doi:10.5194/acpd-14-16691-2014

Atmospheric Chemistry and Physics Discussions

Urban-rural interactions in a South Korean forest: uncertainties in isoprene-OH interactions limit understanding of ozone and secondary organic aerosols production

S. Kim[1], S.-Y. Kim[2], M. Lee[3], H. Shim[3], G. M. Wolfe[4,5], A. B. Guenther[6,7], A. He[1], Y. Hong[2], and J. Han[2]

[1]Department of Earth System Science, School of Physical Sciences, University of California, Irvine, Irvine California, 92697, USA
[2]National Institute Environmental Research, Incheon, South Korea
[3]Department of Earth and Environmental Sciences, Korean University, Seoul, South Korea
[4]Joint Center for Earth Systems Technology, University of Maryland Baltimore County, Baltimore, MD, USA
[5]Atmospheric Chemistry and Dynamics Laboratory, NASA Goddard Space Flight Center, Greenbelt, MD, USA

[6]Atmospheric Sciences and Global Change Division, Pacific Northwest National Laboratory, Richland, WA, USA
[7]Department of Civil and Environmental Engineering, Washington State University, Pullman, WA, USA

Received: 1 May 2014 – Accepted: 10 June 2014 – Published: 24 June 2014

Correspondence to: S. Kim (saewung@uci.edu)

Published by Copernicus Publications on behalf of the European Geosciences Union.

Discussion Paper | Discussion Paper | Discussion Paper | Discussion Paper |

Abstract

Rapid urbanization and economic development in East Asia in past decades has led to photochemical air pollution problems such as excess photochemical ozone and aerosol formation. Asian megacities such as Seoul, Tokyo, Shanghai, Gangzhou, and Beijing are surrounded by densely forested areas and recent research has consistently demonstrated the importance of biogenic volatile organic compounds from vegetation in determining oxidation capacity in the suburban Asian megacity regions. Uncertainties in constraining tropospheric oxidation capacity, dominated by hydroxyl radical concentrations, undermine our ability to assess regional photochemical air pollution problems. We present an observational dataset of CO, NO_x, SO_2, ozone, HONO, and VOCs (anthropogenic and biogenic) from Taehwa Research Forest (TRF) near the Seoul Metropolitan Area (SMA) in early June 2012. The data show that TRF is influenced both by aged pollution and fresh BVOC emissions. With the dataset, we diagnose HO_x (OH, HO_2, and RO_2) distributions calculated with the University of Washington Chemical Box Model (UWCM v 2.1). Uncertainty from unconstrained HONO sources and radical recycling processes highlighted in recent studies is examined using multiple model simulations with different model constraints. The results suggest that (1) different model simulation scenarios cause systematic differences in HO_x distributions especially OH levels (up to 2.5 times) and (2) radical destruction ($HO_2 + HO_2$ or $HO_2 + RO_2$) could be more efficient than radical recycling (HO_2+NO) especially in the afternoon. Implications of the uncertainties in radical chemistry are discussed with respect to ozone-VOC-NO_x sensitivity and oxidation product formation rates. Overall, the VOC limited regime in ozone photochemistry is predicted but the degree of sensitivity can significantly vary depending on the model scenarios. The model results also suggest that RO_2 levels are positively correlated with OVOCs production that is not routinely constrained by observations. These unconstrained OVOCs can cause higher than expected OH loss rates (missing OH reactivity) and secondary organic aerosol formation. The series of modeling experiments constrained by observations strongly urge observational constraint

of the radical pool to enable precise understanding of regional photochemical pollution problems in the East Asian megacity region.

1 Introduction

NO_x ($NO + NO_2$) and VOCs are two important precursors that drive HO_x radical cycles as shown in Fig. 1. Peroxy radical (HO_2 and RO_2) chemistry becomes the backbone of OH recycling. In addition, subsequent interactions with peroxy radicals and NO_x ($NO + NO_2$) produce ozone and oxygenated VOCs (OVOCs) that are precursors for secondary organic aerosols. In summary, in the presence of NO_x, VOC oxidation processes recycle OH and produce photochemical oxidation products. This reaction cycle is highly non-linear. For example, excess NO_2 may expedite nitric acid formation (Reaction R1), limiting ozone production. In the same context, excess VOCs may expedite peroxy radical production (Reaction R2), which limits OH regeneration from peroxy radicals.

$$OH + NO_2 + M \rightarrow HNO_3 + M \quad \text{(R1)}$$

$$HO_2 + RO_2 \rightarrow ROOH \quad \text{(R2)}$$

The non-linearity in tropospheric photochemistry has been relatively well studied in the urban regions of developed countries and applied in ozone reduction policy. The Los Angeles Metropolitan Area has accomplished significant ozone reduction by implementing aggressive emission reductions of both NO_x and VOC especially from mobile sources (Ryerson et al., 2013). The remarkable ozone abatement was possible due to the fact that there is no significant pollution transport from other metropolitan areas and no significant natural emission sources especially volatile organic compounds from vegetation (BVOCs; biogenic volatile organic compounds). In the late 80s, Trainer et al. (1987) first demonstrated the importance of isoprene (C_5H_8) as a peroxy radical source that can contribute significant ozone production in rural areas. The importance

of isoprene in ozone production in urban areas has also been highlighted, e.g. in the Atlanta Metropolitan Area (Chameides et al., 1988).

Isoprene is a hemiterpenoid species and is the globally dominant VOC emission from vegetation (Guenther, 2013). Arguably, isoprene is the most frequently studied BVOC from the perspective of atmospheric oxidation processes and their implications for ozone and aerosol formation. However, significant uncertainty hinders assessment of the roles of isoprene in regional and global photochemistry in three fronts. First, there is still significant uncertainty in estimating emission rates from each individual plant species on regional scales (Guenther, 2013). Second, limited isoprene intercomparison results (Barket et al., 2001) suggest that there are large systematic biases among different analytical techniques. Lastly, recent laboratory, theoretical and field observations suggest significant uncertainty in tropospheric isoprene oxidation processes initiated by OH. Until early 2000, it was thought that three first generation isoprene oxidation products (methyl vinyl ketone, methacrolein, and formaldehyde) from OH oxidation were enough to constrain isoprene tropospheric oxidation processes for modeling purposes (e.g. Spaulding et al., 2003). This is an interesting evolution of thoughts considering that Paulson and Seinfeld (1992), one of pioneering works describing isoprene oxidation, clearly claimed that 22 % of first generation isoprene oxidation products from the reaction with OH was not identified and likely included multifunctional C5 compounds. Recent advances in analytical techniques (Kim et al., 2013a) have shown that indeed significant C5-hydroxy carbonyl (e.g. isoprene hydroperxyenals, HPALD) and peroxide compounds are produced as first generation isoprene oxidation products (Crounse et al., 2011; Paulot et al., 2009; Wolfe et al., 2012; Zhao and Zhang, 2004) and are a strong function of NO concentrations (Peeters and Muller, 2010). In general, low to intermediate NO levels (~ 100 pptv or lower), the yields of C5-hydroxy carbonyl compounds become higher. These new findings in the isoprene oxidation process are also closely related with recent findings in unexpectedly high OH concentrations (Hofzumahaus et al., 2009; Lelieveld et al., 2008) and substantial missing OH sinks also known as unexpectedly high OH reactivity in high isoprene environments (Di

Carlo et al., 2004; Edwards et al., 2013; Kim et al., 2011; Lou et al., 2010; Nolscher et al., 2012).

These new findings have significant implications in regional air quality especially in photochemical ozone and SOA production. Despite the strong anthropogenic pollutant emissions in East Asia (China, Japan and South Korea), recent research has shown that isoprene accounts for a major OH chemical sink in suburban areas near Beijing (Ran et al., 2011), the Pearl River Delta region (Lu et al., 2012), and Seoul (Kim et al., 2013d, b). Consequently, modeling studies also clearly show that isoprene contributes significantly to ozone formation in Asian megacity regions. Kim et al. (2013d) reported that simulated ozone levels with isoprene chemistry are up to 30 % higher than ozone simulation without isoprene chemistry using the WRF-Chem model, indicating an urgent need to implement improved isoprene chemistry schemes in these models in order to simulate the unexpected higher levels of OH in isoprene rich environments. This is especially alarming as Hofzumahaus et al. (2009) reported significantly higher (~ 2.6 times at noon) than expected OH levels in the Pearl River Delta region in China. Therefore, the current assessments based on the conventional OH photochemistry could significantly misdiagnose regional air-quality status and mislead policy implementation to reduce photochemical air pollution in the East Asian region. Furthermore, as the importance of BVOC in regional air-quality issues in ozone and SOA formation has been also reported in Europe and North America, the potential uncertainty has significant implications in urban and suburban air quality in general (Zhang et al., 2008a; Sartelet et al., 2012).

We present atmospheric observations of NO_x, CO, VOCs, ozone, and HONO in the Taehwa Research Forest (TRF) in the Seoul Metropolitan Area (SMA), South Korea. We use these data to conduct observationally constrained box model (University of Washington Chemical Box Model; UWCM) calculations to estimate OH concentrations with different sets of observational parameters. We discuss current uncertainty in OH-isoprene photochemistry with perspectives of constraining photochemical ozone production and oxygenated VOCs precursors of secondary organic aerosols.

2 Methods

The Taehwa Research Forest (TRF) is located ~ 35 km from the center of Seoul, South Korea. The TRF is located at the southeastern edge of the Seoul metropolitan Area (SMA, population of ~ 23 million). TRF has a sampling tower located in the middle of a coniferous tree plantation with the canopy height of 18 m (*Pinus koraiensis*) surrounded by a deciduous forest. Kim et al. (2013d) reported CO, NO_x, SO_2, ozone, and VOC observation results along with WRF-Chem assessments of ozone forming potential of isoprene photochemistry. The report found that isoprene was the most dominant OH chemical sink during daytime among the observed trace gases and explained up to 30 % of ozone production. The TRF instrumentation has previously been described by Kim et al. (2013d). Therefore, just brief descriptions of analytical techniques are given in this paper.

2.1 CO, NO_x, SO_2, ozone, VOCs, and meteorological parameters

Thermo Fisher Scientific Enhanced Trace Level Gas Analyzers are used for CO, NO_x, SO_2, and ozone observations. VOC observations are conducted by a High-Sensitivity Proton Transfer Reaction-Mass Spectrometer (PTR-MS, Ionicon GmbH). The atmospheric application of this technique is thoroughly reviewed by de Gouw and Warneke (2007). In addition, the instrument suite at TRF is thoroughly described in (Kim et al., 2013d). PTR-MS can quantify atmospheric VOCs that have higher proton affinity than the proton affinity of H_2O (691 kJ mol^{-1}). Most alkanes have lower proton affinity than water but alkene, aromatic and some oxygenated VOCs have higher proton affinity and are suitable for quantification using PTR-MS (Blake et al., 2009). These compounds are more reactive than alkane compounds so PTR-MS has capability to observe reactive atmospheric compounds in the atmosphere. The TRF PTR-MS system was set to measure acetaldehyde, acetone, acetic acid, isoprene, methylvinylketone (MVK) + methacrolein (MACR), MEK, benzene, xylene (*p*, *m*, and *o*), and monoterpenes (MT). Each compound was set to be monitored for 1 s each resulting in a sample

cycle of 15 s. Meteorological parameters such as temperature and humidity are monitored by LSI LASTEM Meteorological Sensors. All the presented data is from the 15 m sampling (the canopy height is 18 m) line and meteorological sensors collocated at this height.

PTR-MS has an intrinsic limitation that isobaric compounds are all collectively quantified with the same channel (m/z). This limitation particularly becomes an issue for investigating the roles of different isomers of MT and sesquiterpenes (SQTs) in photochemistry. For this reason, we also occasionally collect sorbent cartridge samples to analyze MT and SQT speciation in both ambient air and branch enclosure emissions near the sampling tower. As described in (Kim et al., 2013d), Tenax GR and Carbotrap 5TD packed sorbent cartridges (Markes Int, Llanstrisant, UK) were used for sampling. The sampled cartridges were shipped to National Center for Atmospheric Research (NCAR), Boulder CO, USA for gas chromatography-mass spectrometer (GC-MS) analysis. An Agilent 7890 GC/5975 C Electron Impact Mass Spectrometer (GC-MS/FID) in conjunction with a MARKES Unity1/Ultra thermal desorption system optimized for terpenoid analysis quantifies speciated MT and SQT in the sorbent samples. Cartridge samples are both collected from ambient and branch enclosure air. Ambient samples were collected in the mid-day to early afternoon with a volume of 6 L. Ozone in the ambient air was removed using a Na_2SO_3 filter. Branch enclosure samples were also collected in the mid-day time frame with a volume of 1 L without an ozone filter as zero air was introduced to the branch enclosure.

2.2 HONO quantification

HONO was measured with an ion chromatography (IC) coupled with diffusion scrubber. Air was introduced to diffusion scrubber (Lab solutions Inc., IL, USA) through a 2 m PFA tubing (1/4″ i.d.) at 1.5 L m^{-1} using a filtered orifice restrictor (F-950, air logic, WI, USA). Air flowing through diffusion scrubber interfaced with deionized water, into which HONO was extracted. 50 µL of solution was injected into the IC system through a PEEK loop (Rheodyne, WA, USA) and 6-way valve (EV750-100, Rheodyne, WA,

USA). Eluent was a mixture of Na_2CO_3 and $NaHCO_3$, which was pumped by a HPLC pump (DX-100, Dionex, CA, USA) into a guard column (Ionpax® AG 14, 4 mm × 50 mm, Dionex, CA, USA) and then analytical column (Ionpax® AS 14, 4 mm × 250 mm, Dionex, CA, USA). The column affluent passed through a suppressor (ASRS 300, Dionex, CA, USA) and HONO was detected as nitrite ion in conductivity detector (550, Alltech, IL, USA). The entire measurement processes of sampling, chemical analysis, and data acquisition were controlled by a digital timer and data acquisition software (DSchrom-n, DS science, Korea), by which we obtained two measurements every hour. The system was calibrated using a NO_2^- standard solution (Kanto chemical Co., Inc., Tokyo, Japan) whenever reagents were replaced. The detection limit was 0.15 ppb estimated from 3σ of the lowest working standard. Specific analytical characteristics are described in Simon and Dasgupta (1995) and Takeuchi et al. (2004).

2.3 UWCM box model

UWCM (v.2.1) has the capability to adapt the Master Chemical Mechanism version 3.2 (MCM 3.2) (Jenkins et al., 1997; Saunders et al., 2003) including all the chemical species and reactions. A more detailed model description can be found in Wolfe and Thornton (2011). Recently developed isoprene photo-oxidation mechanisms shown in Archibald et al. (2010) are also incorporated in the model. In addition, Kim et al. (2013c) and Wolfe et al. (2013) applied the model in the identical fashion as used for this study to probe radical distributions using comprehensive observational datasets. This study used the UWCM to simulate the diurnal variations of radical pool ($OH + HO_2 + RO_2$) distributions as observational parameters such as CO, NO_x, ozone, and VOCs are constrained. To fully account for roles of OVOCs in the box model as radical sources, we simulated three consecutive days and presented diurnal variations from the third day. The specific parameters, constrained by observations are listed above.

3 Results

3.1 Observational results

Diurnal averages of observed trace gases (1 June 2012 to 6 June 2012) are shown in Fig. 2. During this period, the weather was mostly clear and the trace gases were observed in the typical ranges observed during the previous summer (Kim et al., 2013b). Regionally, a high pressure system caused a stagnant air pollution event in this period. In the center of Seoul, carbon monoxide was observed in the similar levels during the observed period. On the other hand, the NO_2 level observed in central Seoul was much higher (20–50 ppb) compared with observed levels at TRF. This can be interpreted as due to differences between the chemical lifetime of CO (~ a month) and NO_2 (~ a few hours to a day). The observations also clearly indicate that the TRF is not directly influenced by fresh SMA pollution plumes although the TRF is very close to the Seoul metropolitan area (30 km away from the city center). Similar observations were also reported for other East Asian megacities such as Beijing (Ma et al., 2012), where ~ 30 ppb and ~ 15 ppb of NO_2 were observed at noon in the urban and the rural sites, respectively. In contrast, there were no noticeable differences in CO levels between the urban and rural sites (~ 1–2 ppm). The observed CO, NO_x and SO_2 levels in TRF were much lower than those observed in the suburban regions of Chinese megacities such as Beijing (Ma et al., 2012), Shanghai (Tie et al., 2013), and the Pearl River Delta Region (Lu et al., 2012) and similar with the observed levels in Tokyo, Japan (Yoshino et al., 2012).

Previous VOC observations in the SMA consistently have shown that toluene is the dominant anthropogenic VOC followed by other aromatic compounds such as xylene and benzene (Kim et al., 2012; Na and Kim, 2001). Na and Kim (2001) reported high concentrations of propane from house hold fuel use. However, recent observation results from the photochemical pollution observational network managed by National Institute of Environmental Research (NIER) of South Korea in the SMA clearly indicate that propane levels have declined and are now much lower than the levels previously

observed (NIER, 2010). This is probably caused by the implementation of a policy changing household fuel sources from propane to methane. (Kim et al., 2012) presented detailed aromatic VOC distributions in the SMA from four different urban observational sites. In average, toluene concentrations were observed ~ 7 times higher than the observed levels of xylene and benzene. At the TRF, a similar anthropogenic VOC speciation distribution was observed as shown in Fig. 2. The observed toluene and MEK (methyl ethyl ketone) mixing-ratios were much higher than benzene and xylene. MEK is detected in m/z of 73^+ by PTR-MS. Although methyl glyoxal, an atmospheric VOC oxidation product, is also detected on the same mass, we assumed that 73^+ of m/z signals are mostly from MEK, an anthropogenic VOC, since the temporal variation follows that of anthropogenic VOC such as toluene and xylene. In addition, atmospheric lifetime of methyl glyoxal is much shorter than MEK.

As the observation facility is located in the middle of a pine tree plantation (*Pinus koraiensis*), monoterpenes (MT) are consistently observed. The temporal variation of monoterpenes is affected by the planetary boundary layer evolution with a pattern of higher MT levels during night than those of mid-day as has been often reported in other forest environments (Bryan et al., 2012; Kim et al., 2010), which can be explained by interplays between boundary layer evolution and temperature dependent MT emission. The observed MT and SQT speciation information is summarized in Table 2. Table 2a summarizes branch enclosure sample analysis results and ambient sample analysis results are summarized in Table 2b. In general, observed MT and SQT in the ambient air are consistent with previously observed distributions (Kim et al., 2013d). α-pinene and β-pinene were the dominant monoterpene and longifolene was the only detected SQT species. In contrast, the branch enclosure observation results, reflecting BVOC emission, indicate high emission of very reactive MT and SQT species such as β-myrcene, α-caryophyllene, and β-caryophyllene. The fast oxidation of these highly reactive terpenoid species suppresses the atmospheric presence of the compounds. Therefore, photochemical oxidation processes of these compounds may have been neglected. Investigating emissions and photochemistry of these reactive terpenoid

compounds can constrain potential missing OH reactivity and SOA production from highly oxidized reaction products.

Isoprene is produced from carbon recently fixed through photosynthesis resulting in higher emissions and atmospheric concentrations during the daytime. The temporal variation shown in Fig. 2 reveals an isoprene concentration maximum between 17:00 LT to 20:00 LT. In addition, the ratios of MVK + MACR, major isoprene oxidation products and isoprene at this period, are significantly lower than those of late morning to early afternoon. This may indicate that two distinctive air masses were observed during early afternoon and late afternoon time periods. In general, this pattern is consistently observed at TRF and probably governed by local and regional atmospheric advection systems as described in Ryu et al. (2013). Another possibility is that the reduced vertical mixing and lower photochemical losses at this time of day results in higher isoprene concentrations. The branch enclosure observations demonstrate that isoprene is not emitted from the pine plantation but rather transported from surrounding broadleaf forests. Oak comprises 85 % of broadleaf trees in South Korea (Lim et al., 2011). Lim et al. (2011) quantified isoprene emission rates for five representative oak species in South Korea and report a wide emission range from oaks that are negligible isoprene emitters ($< 0.004\ \mu g\ C\ dw^{-1}\ h^{-1}$; standard emission rates) to others with very high isoprene emission rates of $130\ \mu g\ C\ dw^{-1}\ h^{-1}$.

Contributions from each observed trace gas species towards ambient OH reactivity are shown in Fig. 3. This is calculated as the product of the observed species concentration and its rate constant for reaction with OH. Observed OH reactivity from VOCs are much higher than from other trace gases such as CO, NO_x, SO_2, and ozone. Among the observed VOC species, BVOCs such as isoprene, α-pinene and β-pinene accounted for significantly higher OH reactivity in comparison with the observed AVOCs such as toluene, benzene, xylene and MEK. Isoprene accounts the highest OH reactivity especially during the daytime. This analysis is consistent with reports from other suburban observations from East Asian megacities such as Beijing (Ran et al.,

2011), the PRD region, China (Lou et al., 2010), and the Kinki region Japan (Bao et al., 2010).

HONO levels up to 1 ppb were observed in the early morning and were consistently higher than 0.5 ppb during the daytime. These observed levels are substantially higher than reported observations from forest environments in North America (Ren et al., 2011; Zhou et al., 2011), where NO_x (~ 1 ppb) is substantially lower than the level observed at TRF. Ren et al. (2011) reported 30–60 ppt of HONO at the Blodgett Forest Research Station in the western foothills of the Sierra Nevada Mountains in the late summer of 2007. Zhou et al. (2011) also reported the similar levels of HONO (below 100 ppt) from the PROPHET forest, a mixed hardwood forest in northern Michigan (Pellston, MI). However, significantly higher HONO levels (~ 200 ppt to ~ 2 ppb) were reported by Li et al. (2012) from a rural observational site in the Pearl River Delta region near Guangzhou, where comparable NO_2 levels with TRF were observed. The high HONO levels (a few hundred ppt) especially during the daytime have been consistently reported near Eastern Asian megacities such as Beijing (Li et al., 2012), Shanghai (Hao et al., 2006), and Seoul (Song et al., 2009). Still these are limited datasets and further comprehensive analysis, especially more extensive observation is required. However, two recently proposed HONO production mechanisms may be able to explain the higher levels in the Eastern Asian megacity region. One is HONO production from NO_2 photo-excitation (Wong et al., 2012) as the region usually has high NO_2 concentrations and the other is HONO emission from soil bacteria (Oswald et al., 2013). Oswald et al. (2013) found differences as much as two orders of magnitude in HONO emissions from soil samples from different environments (e.g. pH and nutrient contents). In addition, as most of observations in the East Asia regions were conducted with ion chromatography based methods, more direct HONO quantification techniques such as a chemical ionization mass spectrometry technique (Roberts et al., 2010) need to be used to characterize any potential interferences such a high NO_x environment (e.g. N_2O_5).

3.2 Implications of uncertainties in isoprene-hydroxyl radical interactions in assessments of regional ozone and organic aerosol precursor production

The presented observational results are used to constrain the UWCM box model and evaluate uncertainties in the tropospheric oxidation capacity and how it affects our ability to constrain ozone and secondary aerosol precursor production. The observational results clearly indicate that isoprene is the dominant OH sink among the observed VOCs. In addition, NO concentrations were higher in the 600 to 800 ppt range in the morning. On the other hand, afternoon levels were substantially lower in the 50 to 100 ppt range. The environment provides a unique opportunity to examine implications of isoprene photochemistry in various NO conditions.

We conducted model calculations under seven different scenarios. Each scenario is described in Table 1. The quantitative assessments of the impacts to radical concentrations (OH, HO_2, and RO_2) from unconstrained HONO sources are evaluated by examining the model outcomes of the scenarios with and without constraining observed HONO. To evaluate the impacts of HPALD photolysis and isoprene peroxy radical recycling in the radical pool, each chemical mechanism is selectively constrained by different scenarios. For HPALD chemistry, we adapted two different HPALD formation rate constants published by Peeters et al. (2009) and Crounse et al. (2011). The formation rates from Peeters et al. (2009) is about 40 times faster than those from Crounse et al. (2011) in 298 K. We applied 2.6 of the OH yield from isoprene peroxy radical and HO_2 reactions for the evaluation (Wolfe et al., 2011).

Modeled OH, HO_2, and RO_2 from the five different model scenarios are shown in Fig. 4a. A summary of averaged OH, HO_2, and RO_2 concentrations in the morning (08:00–11:00 LT) and the afternoon (13:00–16:00 LT) from each simulation is shown in Table 3. With respect to the base run results (Scenario I), Scenario III does not cause noticeable differences in radical concentrations. Adapting higher HPALD formation rates (Scenario II) cause significant differences in radical distribution especially in RO_2. This observation is likely caused by the fact that significant isoprene peroxy

radical is converted to HPALD. The higher levels of discrepancy is observe in RO_2 between Scenario I and Scenario II in the afternoon when NO concentrations are observed in low, which efficiently facilitates HPALD formation. Adding HO_2 + isoprene peroxy radical reactions as OH recycling processes (Scenario IV and V) results in significant enhancements in OH and HO_2 with respect to the base run (Scenario I). RO_2 concentrations are calculated in significantly different levels between Scenario IV and V. This can be again accounted by the applications of different HPALD formation rates in the two different model scenarios. The higher level of OH from the additional recycling process causes substantially higher RO_2 formation rates than those from the scenarios without the additional recycling process. The faster HPALD formation in Scenario IV is appeared to cause faster loss of RO_2 resulting in low RO_2 concentrations.

Most striking differences were observed model simulation results with or without constraining observed HONO as shown in Fig. 4b and c. Calculation results from both Scenario VI and VII indicate significantly smaller OH, HO_2, and RO_2 concentrations than the concentrations calculated from the counter parts Scenario I and VI, which are constrained by observed HONO, respectively. Again, this clearly indicates that more thorough evaluations not only impacts of HONO to air quality but also analytical techniques should be followed to precisely constrain photochemical processes in the region.

Two competing chemical reactions (Reactions R3 vs. R4–R6) determine radical distribution regimes.

$$RO_2 + NO \rightarrow RO + NO_2 \quad \text{(R3)}$$

$$RO_2 + HO_2 \rightarrow ROOH + O_2 \quad \text{(R4)}$$

$$RO_2 + RO_2 \rightarrow ROOR + O_2 \quad \text{(R5)}$$

$$HO_2 + HO_2 \rightarrow H_2O_2 + O_2 \quad \text{(R6)}$$

When the rate of Reaction (R3) gets much faster than the sum of reaction rates of Reactions R4–R6 then radical recycling processes become more efficient than radical destruction processes. In this radical recycling regime, OH, a universal tropospheric oxidant, is well buffered to maintain the elevated OH levels. On the other hand, the radical

destruction regime can be defined when the radical recycling rates (Reaction R3) are slower than the radical destruction reaction rates (Reactions R4–R6). The temporal variations of radical-radical reaction rates from the model simulation scenarios are shown in Fig. 5. In general, the radical reaction rates are elevated as much as twice once observed HONO (Scenario VI and VII) is constrained in the model calculations. This is because unaccounted HONO in the model calculations cause significant underestimations in the radical pool ($OH + HO_2 + RO_2$) size with respect to the constrained HONO scenarios as shown in Fig. 4. In addition, as we include recently developed isoprene radical chemistry, the $RO_2 + HO_2$ reaction rates, known for a radical destruction pathway becomes more faster. This is more conspicuous in the afternoon when NO concentration becomes lower. The $RO_2 + HO_2$ reaction rates get higher than those of RO_2 + NO in the afternoon for the Scenario V and IV. This is surprising, as the radical destruction regime is usually associated with low NO_x conditions. Suburban regions of megacities including the TRF in general show high NO_x conditions. However, radical recycling rates are determined by concentrations of NO. The fraction of NO in the NO_x pool is determined by competing reactions between NO_2 photolysis and oxidation reactions of NO by ozone, HO_2, and RO_2 radicals. Once we assume the pseudo-steady state of NO, then NO in NO_x pool can be expressed as

$$[NO] = J_{NO_2}[NO_2]/(k_{NO+O_3}[O_3] + k_{NO+HO_2}[HO_2] + k_{NO+RO_2}[RO_2]) \quad \text{(R7)}$$

This mathematical expression clearly shows that NO levels are dependent on NO_x mostly composed of NO_2. At the same time, the fraction of NO in NO_x is anti-correlated with ozone, HO_2, and RO_2 concentrations. Therefore, the size of the radical pool composed of HO_2 and RO_2 is relevant for determining the fractions of NO in given NO_x levels. High HO_2 and RO_2 are likely observed in high VOC regions such as forested areas. This could cause a smaller fraction of NO in the given NO_x pool so radical recycling gets relatively weaker compared with radical destruction reaction pathways. More quantitative approaches are required to categorize radical reaction pathways rather than qualitative categorization such as high or low NO_x regimes.

High and low NO_x regimes also have been widely used to define ozone production regimes. As NO_x catalyzes ozone production and peroxy radicals expedite NO_x turnover, in general, higher NO_x and VOCs conditions result in higher ozone production. However, non-linearity in photochemistry of ozone production causes a complexity in ozone reduction strategy (Seinfeld, 1989). Conventionally, efficient ozone production can be achieved by the balance between nitric acid production rates (P_{HNO_3}, $OH + NO_2$) and peroxide production rates (P_{ROOH}, $HO_2 + RO_2$ or $P_{H_2O_2}$ $HO_2 + HO_2$) (Sillman and He, 2002). The imbalance will cause ozone production sensitivity towards either NO_x or VOCs. A comprehensive photochemical model analysis (Tonnesen and Dennis, 2000a, b) demonstrated that in a wider range of ozone concentrations, the VOC and NO_x limited regimes can be determined by the ratios of $P_{H_2O_2}$ and P_{HNO_3}. The ratio range ($P_{H_2O_2}/P_{HNO_3}$) of 0.35 is regarded as the border range. In the VOC limited regime ($P_{H_2O_2}/P_{HNO_3} < 0.35$), ozone production is expected to decrease with increasing NO_x and increase with increasing VOCs. In the NO_x limited regime ($P_{H_2O_2}/P_{HNO_3} > 0.35$), ozone production gets efficient with increasing NO_x and is insensitive to changes in VOCs (Sillman and He, 2002). This categorization has guided policy-making processes whether NO_x or VOC controls will be more effective in ozone reduction. A series of modeling studies have been conducted to characterize ozone production regimes in the suburban regions of East Asian megacities and have consistently concluded that the role of isoprene is important in ozone production. However, most of these studies have concluded that East Asian megacity regions are mostly in the VOC limited regime (Tseng et al., 2009; Zhang et al., 2008b; Lim et al., 2011; Cheng et al., 2010; Shao et al., 2009a, b; Xing et al., 2011). Recently, however, a modeling study by Li et al. (2013) in the Pearl River Delta region in China demonstrated the time dependence of ozone production regimes. Specifically, with high NO_x emissions in the morning, the regional ozone production regime is categorized as VOC limited. In contrast, in the afternoon when the highest ozone concentrations are observed, a NO_x limited regime is often found. The obvious issue to be addressed is that all of the above studies neglected how the uncertainty in hydroxyl radical chemistry would affect the ozone

production regime evaluation. In addition, HONO has been rarely constrained by observations in the previous modeling studies. Figure 6 shows the temporal variations of $P_{H_2O_2}/P_{HNO_3}$ from the four different model scenarios. The VOC limited ozone formation regime was observed regardless of the HO_x simulation scenarios. Differences among different scenario are not noticeable in the morning when NO is high but noticeable differences are observed in the afternoon. In general, the model calculation results with faster HPALD formation rates indicate higher $P_{H_2O_2}/P_{HNO_3}$ in the afternoon. The identical tendency was found in the model calculation results without constraining observed HONO (not shown in Fig. 6). This analysis clearly shows that it is difficult to determine the appropriate policy implementation for NO_x or VOC controls to achieve ozone abatement in Asian megaticities without accurate understanding of radical isoprene interactions (e.g. Kim et al., 2013b).

Another unresolved uncertainty in understanding tropospheric OH is its chemical loss rates. The limited observations of OH reactivity in BVOC dominant environments show consistent unaccounted OH chemical loss with observational datasets (Di Carlo et al., 2004; Edwards et al., 2013; Kim et al., 2011; Lou et al., 2010; Nolscher et al., 2012). Two different processes are speculated to cause unaccounted OH loss known as missing OH reactivity: (1) primary emissions of unmeasured or unknown compounds and (2) oxidation products of well-known BVOCs especially isoprene. Most studies conducted in coniferous forests where monoterpenes are dominant primary BVOC emissions have concluded that unmeasured or unknown primary BVOC emissions caused missing OH reactivity (Sinha et al., 2010). On the other hand, studies conducted in isoprene dominant environments in mostly broadleaf or mixed forests concluded the main cause of missing OH reactivity as oxidation products of isoprene (Edwards et al., 2013; Kim et al., 2011). Edwards et al. (2013) presented a thorough analysis on potential impacts of isoprene oxidation products that are not routinely constrained by observations. The authors found significant contributions from secondary oxidation products such as multi-functional oxygenated compounds. Figure 7a shows the temporal variations of total OH reactivity calculated from five different model

scenarios (I through V). The highest and the lowest OH reactivity levels were predicted from model calculations of Scenario V and Scenario II, respectively. This observation is directly correlated with calculated RO_2 levels as the lowest and highest RO_2 levels were calculated from Scenario II and Scenario V, respectively. Since VOC precursors and trace gases were all constrained by observations in the model calculations, the differences in model calculated OH reactivity should be mainly caused by the oxidation products of VOCs. This can be confirmed by the comparisons of model calculated formaldehyde concentrations from Scenario II and V as formaldehyde is a dominant oxidation product of isoprene. The differences in formaldehyde levels suggest differences in OH reactivity levels from OVOCs in each model simulation. In summary, uncertainty in radical distributions especially RO_2 levels is directly propagated into uncertainty in OVOC formation.

These calculated results provide an upper limit of potential contributions from the oxidation products of the constrained VOC precursors considering that the box-model does not consider dry-deposition processes as Karl et al. (2010) and (Edwards et al., 2013) suggested that there is significant uncertainty associated with the parameterizations of dry deposition especially OVOCs. Still, this analysis suggests that significant missing OH reactivity (~ up to factor of two to three) can be found without constraining OVOCs. OVOCs, especially multi-functional highly oxidized compounds are precursors for secondary organic aerosols (VOCs). Therefore, uncertainty surrounding missing OH reactivity significantly undermines our ability to constrain SOA formation and aerosol growth.

4 Summary

We presented trace gas observation results from the TRF near the SMA. The dataset provides important constraints to evaluate the HO_x pool at the site where both anthropogenic and biogenic influences become important factors in determining oxidation capacity. Although the site is in the vicinity of a megacity with 25 million people, isoprene

accounted for most of the OH loss from observed atmospheric hydrocarbon species during the observational period in early June 2012. In addition, observed NO_x levels were substantially lower than observed values in the center of the SMA. These observations indicate that impacts of aged pollution on BVOC photochemistry and aerosol formation can be observed at the TRF.

Seven different model calculation scenarios are employed to investigate the radical (OH, HO_2, and RO_2) distributions using the UWCM box-model as summarized in Table 1. The observed trace gas data were constrained and the photochemical mechanisms (MCM 3.2) of seven VOC species observed in high levels at the TRF were integrated. The different scenarios result in a wider range of OH, HO_2, and RO_2 distributions. Unconstrained HONO sources are also appeared to cause a quite high level of underestimation in a radical pool ($OH + HO_2 + RO_2$). A larger difference is observed in OH simulations (up to three times) than simulations for HO_2 and RO_2 (up to twice). OH is simulated in much higher levels with the consideration of an additional OH recycling channel from isoprene peroxy radical + HO_2 reactions and fast HPALD formation chemistry (Peeters et al., 2009). On the other hand, the RO_2 simulations indicate contrary results as HPALD formation depletes the RO_2 pool, which mostly composed by isoprene peroxy radicals. These results suggest that HO_2 and RO_2 observations can provide pivotal information about radical recycling (Kim et al., 2013c; Wolfe et al., 2013). More studies on characterizing existing techniques to quantify HO_2 (Fuchs et al., 2011) and developing new techniques (Horstjann et al., 2013) are needed. In addition, the simulations with recently developed isoprene photo-oxidation chemistry show that radical termination processes (e.g. peroxide formation) get more efficient than radical recycling processes in the afternoon. This may come as a surprise as in general we expect the high NO_x conditions in the suburban regions of a megacity to have effective radical recycling. However, the critical factor determining competing reaction channels of recycling and peroxide formation is NO concentrations. Ratios of NO to NO_2 are not only correlated with NO_2 concentrations and photolysis constants but also anti-correlated with RO_2, HO_2 and ozone concentrations and relevant kinetic constants as

shown in (R6). Therefore, a semi-quantitative term such as the high "NO_x" regime is not a proper term to define radical recycle regimes especially in high radical environments (e.g. HO_2 and RO_2) such as forest environments.

These uncertainties surrounding the radical pool size and distribution directly affect our ability for constraining photochemical ozone and SOA production. The non-linear response of ozone production to NO_x and VOC abundances are determined by OH, HO_2, RO_2 and NO_2 concentrations. Regardless of which scenario we adapt, the TRF photochemical state appears to be a VOC limited ozone production regime. However, morning and afternoon show a very strong contrast with morning having a stronger degree of VOC limitation, which is defined by a stronger nitric acid formation in comparison with peroxide formation. In addition, a noticeable range of VOC sensitivity was calculated from the four different model scenarios especially in the afternoon. These analysis results, therefore, strongly indicate that uncertainty in radical photochemistry directly propagates in policy-making processes in effectiveness of NO_x or VOC controls in ozone reduction. In addition, OVOC production is predicted to significantly vary depending on the model simulation scenarios. As the fate of these OVOCs is uncertain and can include deposition, photolysis, or condensation, the implications of the uncertainty in OVOC production caused by the uncertainty in radical photochemistry should be addressed.

Acknowledgements. This research is financially supported by National Institute of Environmental Research of South Korea. The authors appreciate logistical supports from the research and supporting staff at Taehwa Research Forest operated by Seoul National University.

References

Bao, H., Shrestha, K. L., Kondo, A., Kaga, A., and Inoue, Y.: Modeling the influence of biogenic volatile organic compound emissions on ozone concentration during summer season in the Kinki region of Japan, Atmos. Environ., 44, 421–431, doi:10.1016/J.Atmosenv.2009.10.021, 2010.

Barket, D. J., Hurst, J. M., Couch, T. L., Colorado, A., Shepson, P. B., Riemer, D. D., Hills, A. J., Apel, E. C., Hafer, R., Lamb, B. K., Westberg, H. H., Farmer, C. T., Stabenau, E. R., and Zika, R. G.: Intercomparison of automated methodologies for determination of ambient isoprene during the PROPHET 1998 summer campaign, J. Geophys. Res.-Atmos., 106, 24301–24313, doi:10.1029/2000jd900562, 2001.

Blake, R. S., Monks, P. S., and Ellis, A. M.: Proton-transfer reaction mass spectrometry, Chem. Rev., 109, 861–896, 2009.

Bryan, A. M., Bertman, S. B., Carroll, M. A., Dusanter, S., Edwards, G. D., Forkel, R., Griffith, S., Guenther, A. B., Hansen, R. F., Helmig, D., Jobson, B. T., Keutsch, F. N., Lefer, B. L., Pressley, S. N., Shepson, P. B., Stevens, P. S., and Steiner, A. L.: In-canopy gas-phase chemistry during CABINEX 2009: sensitivity of a 1-D canopy model to vertical mixing and isoprene chemistry, Atmos. Chem. Phys., 12, 8829–8849, doi:10.5194/acp-12-8829-2012, 2012.

Chameides, W. L., Lindsay, R. W., Richardson, J., and Kiang, C. S.: The role of biogenic hydrocarbons in urban photochemical smog – Atlanta as a case-study, Science, 241, 1473–1475, 1988.

Cheng, H. R., Guo, H., Saunders, S. M., Lam, S. H. M., Jiang, F., Wang, X. M., Simpson, I. J., Blake, D. R., Louie, P. K. K., and Wang, T. J.: Assessing photochemical ozone formation in the Pearl River Delta with a photochemical trajectory model, Atmos. Environ., 44, 4199–4208, doi:10.1016/J.Atmosenv.2010.07.019, 2010.

Crounse, J. D., Paulot, F., Kjaergaard, H. G., and Wennberg, P. O.: Peroxy radical isomerization in the oxidation of isoprene, Phys. Chem. Chem. Phys., 13, 13607–13613, doi:10.1039/C1cp21330j, 2011.

de Gouw, J. and Warneke, C.: Measurements of volatile organic compounds in the earths atmosphere using proton-transfer-reaction mass spectrometry, Mass Spectrom. Rev., 26, 223–257, 2007.

Di Carlo, P., Brune, W. H., Martinez, M., Harder, H., Lesher, R., Ren, X. R., Thornberry, T., Carroll, M. A., Young, V., Shepson, P. B., Riemer, D., Apel, E., and Campbell, C.: Missing OH reactivity in a forest: evidence for unknown reactive biogenic VOCs, Science, 304, 722–725, doi:10.1126/Science.1094392, 2004.

Edwards, P. M., Evans, M. J., Furneaux, K. L., Hopkins, J., Ingham, T., Jones, C., Lee, J. D., Lewis, A. C., Moller, S. J., Stone, D., Whalley, L. K., and Heard, D. E.: OH reactivity in a South East Asian tropical rainforest during the Oxidant and Particle Photochemical Pro-

cesses (OP3) project, Atmos. Chem. Phys., 13, 9497–9514, doi:10.5194/acp-13-9497-2013, 2013.
Fuchs, H., Bohn, B., Hofzumahaus, A., Holland, F., Lu, K. D., Nehr, S., Rohrer, F., and Wahner, A.: Detection of HO_2 by laser-induced fluorescence: calibration and interferences from RO_2 radicals, Atmos. Meas. Tech., 4, 1209–1225, doi:10.5194/amt-4-1209-2011, 2011.
Guenther, A.: Biological and chemical diversity of biogenic volatile organic emissions into the atmosphere, Atmospheric Sciences, 2013, 786290, doi:10.1155/2013/786290, 2013.
Hao, N., Zhou, B., Chen, D., and Chen, L. M.: Observations of nitrous acid and its relative humidity dependence in Shanghai, J. Environ. Sci.-China, 18, 910–915, doi:10.1016/S1001-0742(06)60013-2, 2006.
Hofzumahaus, A., Rohrer, F., Lu, K. D., Bohn, B., Brauers, T., Chang, C. C., Fuchs, H., Holland, F., Kita, K., Kondo, Y., Li, X., Lou, S. R., Shao, M., Zeng, L. M., Wahner, A., and Zhang, Y. H.: Amplified trace gas removal in the troposphere, Science, 324, 1702–1704, doi:10.1126/science.1164566, 2009.
Horstjann, M., Andrés Hernández, M. D., Nenakhov, V., Chrobry, A., and Burrows, J. P.: Peroxy radical detection for airborne atmospheric measurements using absorption spectroscopy of NO_2, Atmos. Meas. Tech., 7, 1245–1257, doi:10.5194/amt-7-1245-2014, 2014.
Karl, T., Harley, P., Emmons, L., Thornton, B., Guenther, A., Basu, C., Turnipseed, A., and Jardine, K.: Efficient atmospheric cleansing of oxidized organic trace gases by vegetation, Science, 330, 816–819, doi:10.1126/Science.1192534, 2010.
Kim, K. H., Ho, D. X., Park, C. G., Ma, C. J., Pandey, S. K., Lee, S. C., Jeong, H. J., and Lee, S. H.: Volatile organic compounds in ambient air at four residential locations in Seoul, Korea, Environ. Eng. Sci., 29, 875–889, doi:10.1089/Ees.2011.0280, 2012.
Kim, S., Karl, T., Guenther, A., Tyndall, G., Orlando, J., Harley, P., Rasmussen, R., and Apel, E.: Emissions and ambient distributions of Biogenic Volatile Organic Compounds (BVOC) in a ponderosa pine ecosystem: interpretation of PTR-MS mass spectra, Atmos. Chem. Phys., 10, 1759–1771, doi:10.5194/acp-10-1759-2010, 2010.
Kim, S., Guenther, A., Karl, T., and Greenberg, J.: Contributions of primary and secondary biogenic VOC tototal OH reactivity during the CABINEX (Community Atmosphere-Biosphere INteractions Experiments)-09 field campaign, Atmos. Chem. Phys., 11, 8613–8623, doi:10.5194/acp-11-8613-2011, 2011.

Kim, S., Guenther, A., and Apel, E.: Quantitative and qualitative sensing techniques for biogenic volatile organic compounds and their oxidation products, Environ. Sci.-Proc. Imp., 15, 1301–1314, doi:10.1039/C3em00040k, 2013a.
Kim, S., Lee, M., Kim, S., Choi, S., Seok, S., and Kim, S.: Photochemical characteristics of high and low ozone episodes observed in the Taehwa Forest observatory (TFO) in June 2011 near Seoul, South Korea, Asia-Pacific J. Atmos. Sci., 49, 325–331, doi:10.1007/S13143-013-0031-0, 2013b.
Kim, S., Wolfe, G. M., Mauldin, L., Cantrell, C., Guenther, A., Karl, T., Turnipseed, A., Greenberg, J., Hall, S. R., Ullmann, K., Apel, E., Hornbrook, R., Kajii, Y., Nakashima, Y., Keutsch, F. N., DiGangi, J. P., Henry, S. B., Kaser, L., Schnitzhofer, R., Graus, M., Hansel, A., Zheng, W., and Flocke, F. F.: Evaluation of HO_x sources and cycling using measurement-constrained model calculations in a 2-methyl-3-butene-2-ol (MBO) and monoterpene (MT) dominated ecosystem, Atmos. Chem. Phys., 13, 2031–2044, doi:10.5194/acp-13-2031-2013, 2013c.
Kim, S. Y., Jiang, X. Y., Lee, M., Turnipseed, A., Guenther, A., Kim, J. C., Lee, S. J., and Kim, S.: Impact of biogenic volatile organic compounds on ozone production at the Taehwa Research Forest near Seoul, South Korea, Atmos. Environ., 70, 447–453, doi:10.1016/J.Atmosenv.2012.11.005, 2013d.
Lelieveld, J., Butler, T. M., Crowley, J. N., Dillon, T. J., Fischer, H., Ganzeveld, L., Harder, H., Lawrence, M. G., Martinez, M., Taraborrelli, D., and Williams, J.: Atmospheric oxidation capacity sustained by a tropical forest, Nature, 452, 737–740, 2008.
Li, X., Brauers, T., Häseler, R., Bohn, B., Fuchs, H., Hofzumahaus, A., Holland, F., Lou, S., Lu, K. D., Rohrer, F., Hu, M., Zeng, L. M., Zhang, Y. H., Garland, R. M., Su, H., Nowak, A., Wiedensohler, A., Takegawa, N., Shao, M., and Wahner, A.: Exploring the atmospheric chemistry of nitrous acid (HONO) at a rural site in Southern China, Atmos. Chem. Phys., 12, 1497–1513, doi:10.5194/acp-12-1497-2012, 2012.
Li, Y., Lau, A. K. H., Fung, J. C. H., Zheng, J. Y., and Liu, S. C.: Importance of NO_x control for peak ozone reduction in the Pearl River Delta region, J. Geophys. Res.-Atmos., 118, 9428–9443, doi:10.1002/Jgrd.50659, 2013.
Lim, Y. J., Armendariz, A., Son, Y. S., and Kim, J. C.: Seasonal variations of isoprene emissions from five oak tree species in East Asia, Atmos. Environ., 45, 2202–2210, doi:10.1016/J.Atmosenv.2011.01.066, 2011.

Lou, S., Holland, F., Rohrer, F., Lu, K., Bohn, B., Brauers, T., Chang, C.C., Fuchs, H., Häseler, R., Kita, K., Kondo, Y., Li, X., Shao, M., Zeng, L., Wahner, A., Zhang, Y., Wang, W., and Hofzumahaus, A.: Atmospheric OH reactivities in the Pearl River Delta – China in summer 2006: measurement and model results, Atmos. Chem. Phys., 10, 11243–11260, doi:10.5194/acp-10-11243-2010, 2010.

Lu, K. D., Rohrer, F., Holland, F., Fuchs, H., Bohn, B., Brauers, T., Chang, C. C., Häseler, R., Hu, M., Kita, K., Kondo, Y., Li, X., Lou, S. R., Nehr, S., Shao, M., Zeng, L. M., Wahner, A., Zhang, Y. H., and Hofzumahaus, A.: Observation and modelling of OH and HO_2 concentrations in the Pearl River Delta 2006: a missing OH source in a VOC rich atmosphere, Atmos. Chem. Phys., 12, 1541–1569, doi:10.5194/acp-12-1541-2012, 2012.

Ma, J. Z., Wang, W., Chen, Y., Liu, H. J., Yan, P., Ding, G. A., Wang, M. L., Sun, J., and Lelieveld, J.: The IPAC-NC field campaign: a pollution and oxidization pool in the lower atmosphere over Huabei, China, Atmos. Chem. Phys., 12, 3883–3908, doi:10.5194/acp-12-3883-2012, 2012.

Na, K. and Kim, Y. P.: Seasonal characteristics of ambient volatile organic compounds in Seoul, Korea, Atmos. Environ., 35, 2603–2614, doi:10.1016/S1352-2310(00)00464-7, 2001.

NIER: Annual Report for Atmospheric Environment, National Insititute of Environmetal Resarch, The Ministry of Environment, Seoul, South Korea, 2010.

Nölscher, A. C., Williams, J., Sinha, V., Custer, T., Song, W., Johnson, A. M., Axinte, R., Bozem, H., Fischer, H., Pouvesle, N., Phillips, G., Crowley, J. N., Rantala, P., Rinne, J., Kulmala, M., Gonzales, D., Valverde-Canossa, J., Vogel, A., Hoffmann, T., Ouwersloot, H. G., Vilà-Guerau de Arellano, J., and Lelieveld, J.: Summertime total OH reactivity measurements from boreal forest during HUMPPA-COPEC 2010, Atmos. Chem. Phys., 12, 8257–8270, doi:10.5194/acp-12-8257-2012, 2012.

Oswald, R., Behrendt, T., Ermel, M., Wu, D., Su, H., Cheng, Y., Breuninger, C., Moravek, A., Mougin, E., Delon, C., Loubet, B., Pommerening-Roser, A., Sorgel, M., Poschl, U., Hoffmann, T., Andreae, M. O., Meixner, F. X., and Trebs, I.: HONO emissions from soil bacteria as a major source of atmospheric reactive nitrogen, Science, 341, 1233–1235, doi:10.1126/Science.1242266, 2013.

Paulot, F., Crounse, J. D., Kjaergaard, H. G., Kroll, J. H., Seinfeld, J. H., and Wennberg, P. O.: Isoprene photooxidation: new insights into the production of acids and organic nitrates, Atmos. Chem. Phys., 9, 1479–1501, doi:10.5194/acp-9-1479-2009, 2009.

Paulson, S. E. and Seinfeld, J. H.: Development and evaluation of a photooxidation mechanism for isoprene, J. Geophys. Res., 97, 20703–20715, 1992.

Peeters, J. and Muller, J. F.: HO_x radical regeneration in isoprene oxidation via peroxy radical isomerisations. II: experimental evidence and global impact, Phys. Chem. Chem. Phys., 12, 14227–14235, doi:10.1039/C0cp00811g, 2010.

Ran, L., Zhao, C. S., Xu, W. Y., Lu, X. Q., Han, M., Lin, W. L., Yan, P., Xu, X. B., Deng, Z. Z., Ma, N., Liu, P. F., Yu, J., Liang, W. D., and Chen, L. L.: VOC reactivity and its effect on ozone production during the HaChi summer campaign, Atmos. Chem. Phys., 11, 4657–4667, doi:10.5194/acp-11-4657-2011, 2011.

Ren, X., Sanders, J. E., Rajendran, A., Weber, R. J., Goldstein, A. H., Pusede, S. E., Browne, E. C., Min, K.-E., and Cohen, R. C.: A relaxed eddy accumulation system for measuring vertical fluxes of nitrous acid, Atmos. Meas. Tech., 4, 2093–2103, doi:10.5194/amt-4-2093-2011, 2011.

Ryerson, T. B., Andrews, A. E., Angevine, W. M., Bates, T. S., Brock, C. A., Cairns, B., Cohen, R. C., Cooper, O. R., de Gouw, J. A., Fehsenfeld, F. C., Ferrare, R. A., Fischer, M. L., Flagan, R. C., Goldstein, A. H., Hair, J. W., Hardesty, R. M., Hostetler, C. A., Jimenez, J. L., Langford, A. O., McCauley, E., McKeen, S. A., Molina, L. T., Nenes, A., Oltmans, S. J., Parrish, D. D., Pederson, J. R., Pierce, R. B., Prather, K., Quinn, P. K., Seinfeld, J. H., Senff, C. J., Sorooshian, A., Stutz, J., Surratt, J. D., Trainer, M., Volkamer, R., Williams, E. J., and Wofsy, S. C.: The 2010 California Research at the Nexus of Air Quality and Climate Change (CalNex) field study, J. Geophys. Res.-Atmos., 118, 5830–5866, doi:10.1002/Jgrd.50331, 2013.

Sartelet, K. N., Couvidat, F., Seigneur, C., and Roustan, Y.: Impact of biogenic emissions on air quality over Europe and North America, Atmos. Environ., 53, 131–141, doi:10.1016/J.Atmosenv.2011.10.046, 2012.

Seinfeld, J. H.: Urban air-pollution – state of the science, Science, 243, 745–752, doi:10.1126/Science.243.4892.745, 1989.

Shao, M., Lu, S. H., Liu, Y., Xie, X., Chang, C. C., Huang, S., and Chen, Z. M.: Volatile organic compounds measured in summer in Beijing and their role in ground-level ozone formation, J. Geophys. Res.-Atmos., 114, D00g06, doi:10.1029/2008jd010863, 2009a.

Shao, M., Zhang, Y. H., Zeng, L. M., Tang, X. Y., Zhang, J., Zhong, L. J., and Wang, B. G.: Ground-level ozone in the Pearl River Delta and the roles of VOC and NO(x) in its production, J. Environ. Manage., 90, 512–518, doi:10.1016/j.jenvman.2007.12.008, 2009b.

Sillman, S. and He, D.: Some theoretical results concerning O_3-NO_x-VOC chemistry and NO_x-VOC indicators, J. Geophys. Res., 107, 4659, doi:10.1029/2001JD001123, 2002.

Sinha, V., Williams, J., Lelieveld, J., Ruuskanen, T. M., Kajos, M. K., Patokoski, J., Hellen, H., Hakola, H., Mogensen, D., Boy, M., Rinne, J., and Kulmala, M.: OH reactivity measurements within a boreal forest: evidence for unknown reactive emissions, Environ. Sci. Technol., 44, 6614–6620, doi:10.1021/Es101780b, 2010.

Song, C. H., Park, M. E., Lee, E. J., Lee, J. H., Lee, B. K., Lee, D. S., Kim, J., Han, J. S., Moon, K. J., and Kondo, Y.: Possible particulate nitrite formation and its atmospheric implications inferred from the observations in Seoul, Korea, Atmos. Environ., 43, 2168–2173, doi:10.1016/J.Atmosenv.2009.01.018, 2009.

Tie, X., Geng, F., Guenther, A., Cao, J., Greenberg, J., Zhang, R., Apel, E., Li, G., Weinheimer, A., Chen, J., and Cai, C.: Megacity impacts on regional ozone formation: observations and WRF-Chem modeling for the MIRAGE-Shanghai field campaign, Atmos. Chem. Phys., 13, 5655–5669, doi:10.5194/acp-13-5655-2013, 2013.

Tonnesen, G. S. and Dennis, R. L.: Analysis of radical propagation efficiency to assess ozone sensitivity to hydrocarbons and NO_x 1. Local indicators of instantaneous odd oxygen production sensitivity, J. Geophys. Res.-Atmos., 105, 9213–9225, doi:10.1029/1999jd900371, 2000a.

Tonnesen, G. S. and Dennis, R. L.: Analysis of radical propagation efficiency to assess ozone sensitivity to hydrocarbons and NO_x 2. Long-lived species as indicators of ozone concentration sensitivity, J. Geophys. Res.-Atmos., 105, 9227–9241, doi:10.1029/1999jd900372, 2000b.

Trainer, M., Williams, E., Parrish, D. D., Buhr, M. P., Allwine, E. J., Westberg, H., Fehsenfeld, F. C., and Liu, S. C.: Models and observations of the impact of natural hydrocarbons on rural ozone, Nature, 329, 705–707, 1987.

Tseng, K. H., Wang, J. L., Cheng, M. T., and Tsuang, B. J.: Assessing the relationship between air mass age and summer ozone episodes based on photochemical indices, Aerosol Air Qual. Res., 9, 149–171, 2009.

VandenBoer, T., Murphy, J. G., Roberts, J. M., Middlebrook, A. M., Brock, C., Lerner, B. M., Wolfe, D. E., Williams, E., Brown, S. S., Warneke, C., De Gouw, J., Wagner, N. L., Young, C. C., Dube, W. P., Bahreini, R., Riedel, T., Thornton, J. A., Ozturk, F., Keene, W., Maben, J. R., Pszenny, A., Kim, S., Grossberg, N., and Lefer, B.: Understanding the role

of the ground surface in HONO vertical structure: high resolution vertical profiles during NACHTT-11, J. Geophys. Res.-Atmos., 118, 10,155–10,171, doi:10.1002/jgrd.50721, 2013.

Wolfe, G. M. and Thornton, J. A.: The Chemistry of Atmosphere-Forest Exchange (CAFE) Model – Part 1: Model description and characterization, Atmos. Chem. Phys., 11, 77–101, doi:10.5194/acp-11-77-2011, 2011.

Wolfe, G. M., Crounse, J. D., Parrish, J. D., St Clair, J. M., Beaver, M. R., Paulot, F., Yoon, T. P., Wennberg, P. O., and Keutsch, F. N.: Photolysis, OH reactivity and ozone reactivity of a proxy for isoprene-derived hydroperoxyenals (HPALDs), Phys. Chem. Chem. Phys., 14, 7276–7286, 2012.

Wolfe, G. M., Cantrell, C., Kim, S., Mauldin III, R. L., Karl, T., Harley, P., Turnipseed, A., Zheng, W., Flocke, F., Apel, E. C., Hornbrook, R. S., Hall, S. R., Ullmann, K., Henry, S. B., DiGangi, J. P., Boyle, E. S., Kaser, L., Schnitzhofer, R., Hansel, A., Graus, M., Nakashima, Y., Kajii, Y., Guenther, A., and Keutsch, F. N.: Missing peroxy radical sources within a summertime ponderosa pine forest, Atmos. Chem. Phys., 14, 4715–4732, doi:10.5194/acp-14-4715-2014, 2014.

Wong, K. W., Tsai, C., Lefer, B., Haman, C., Grossberg, N., Brune, W. H., Ren, X., Luke, W., and Stutz, J.: Daytime HONO vertical gradients during SHARP 2009 in Houston, TX, Atmos. Chem. Phys., 12, 635–652, doi:10.5194/acp-12-635-2012, 2012.

Xing, J., Wang, S. X., Jang, C., Zhu, Y., and Hao, J. M.: Nonlinear response of ozone to precursor emission changes in China: a modeling study using response surface methodology, Atmos. Chem. Phys., 11, 5027–5044, doi:10.5194/acp-11-5027-2011, 2011.

Yoshino, A., Nakashima, Y., Miyazaki, K., Kato, S., Suthawaree, J., Shimo, N., Matsunaga, S., Chatani, S., Apel, E., Greenberg, J., Guenther, A., Ueno, H., Sasaki, H., Hoshi, J., Yokota, H., Ishii, K., and Kajii, Y.: Air quality diagnosis from comprehensive observations of total OH reactivity and reactive trace species in urban central Tokyo, Atmos. Environ., 49, 51–59, doi:10.1016/J.Atmosenv.2011.12.029, 2012.

Zhang, Y., Hu, X. M., Leung, L. R., and Gustafson, W. I.: Impacts of regional climate change on biogenic emissions and air quality, J. Geophys. Res.-Atmos., 113, D18310, doi:10.1029/2008jd009965, 2008a.

Zhang, Y. H., Su, H., Zhong, L. J., Cheng, Y. F., Zeng, L. M., Wang, X. S., Xiang, Y. R., Wang, J. L., Gao, D. F., Shao, M., Fan, S. J., and Liu, S. C.: Regional ozone pollution and observation-based approach for analyzing ozone-precursor

relationship during the PRIDE-PRD2004 campaign, Atmos. Environ., 42, 6203–6218, doi:10.1016/J.Atmosenv.2008.05.002, 2008b.
Zhao, J. and Zhang, R. Y.: Proton transfer reaction rate constants between hydronium ion (H_3O^+) and volatile organic compounds, Atmos. Environ., 38, 2177–2185, 2004.
Zhou, X. L., Zhang, N., TerAvest, M., Tang, D., Hou, J., Bertman, S., Alaghmand, M., Shepson, P. B., Carroll, M. A., Griffith, S., Dusanter, S., and Stevens, P. S.: Nitric acid photolysis on forest canopy surface as a source for tropospheric nitrous acid, Nat. Geosci., 4, 440–443, doi:10.1038/Ngeo1164, 2011.

Table 1. A summary of critical differences in input parameters for four different model simulation scenarios presented in this study.

	HPALD Chemistry	α^*	Observational Constraints
Scenario I	No	0	All
Scenario II	Peeters et al. (2009)	0	All
Scenario III	Crounse et al. (2011)	0	All
Scenario IV	Peeters et al. (2009)	2.6	All
Scenario V	Crounse et al. (2011)	2.6	All
Scenario VI	No	0	All but HONO
Scenario VII	Peeters et al. (2009)	2.6	All but HONO

* α is an OH yield from reactions between an isoprene peroxy radical and HO_2.

Table 2. Terpenoid speciation analysis results from GC-MS (a) branch enclosure and (b) ambient air samples.

(a) Terpenoids	*Composition (%)	Speciation	*Composition (%)
Isoprene	0.5		
Monoterpenes	92.9	α-pinene	36.7
		camphene	13.1
		β-pinene	12.0
		β-myrcene	27.7
		α-terpinolene	1.9
		d-limonene	8.6
Sesquiterpenes	6.6	β-caryophyllene	53.2
		α-caryophyllene	46.8
(b)			
Monoterpenes	98.6	α-pinene	38.8
		β-piene	36.5
		camphene	13.5
		d-limonene	11
Sesquiterpenes	1.4	longifolene	100

* Composition is calculated based on the mixing ratio scale.

Table 3. A summary for radical distributions from the observationally constrained box-model simulation results.

	OH		HO_2		RO_2		Constraints
Local Time	8:00–12:00	13:00–16:00	8:00–12:00	13:00–16:00	8:00–12:00	13:00–16:00	
Scenario I	3.85×10^6	3.08×10^6	4.10×10^8	7.02×10^8	3.65×10^8	1.14×10^9	All
Scenario II	3.99×10^6	3.69×10^6	3.99×10^8	7.86×10^8	3.51×10^8	9.62×10^8	All
Scenario III	3.86×10^6	3.13×10^6	4.09×10^8	7.09×10^8	3.64×10^8	1.12×10^9	All
Scenario IV	4.27×10^6	4.49×10^6	4.29×10^8	8.70×10^8	3.66×10^8	1.06×10^9	All
Scenario V	4.21×10^6	4.52×10^6	4.55×10^8	8.55×10^8	3.86×10^8	1.28×10^9	All
Scenario VI	1.61×10^6	1.61×10^6	1.95×10^8	4.82×10^8	1.75×10^8	7.25×10^8	All but HONO
Scenario VII	1.82×10^6	2.55×10^6	2.09×10^8	6.07×10^8	1.80×10^8	7.00×10^8	All but HONO

unit: molecules cm^{-3}

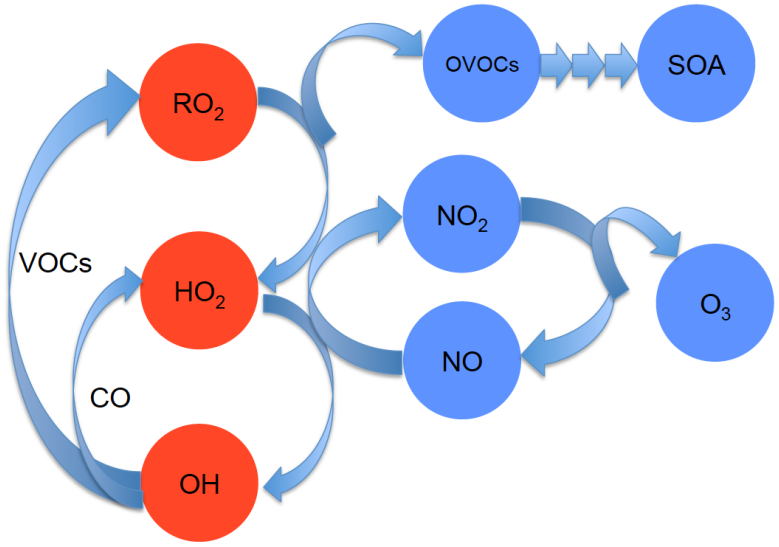

Figure 1. A summary of HO_x-NO_x-VOC photochemical reaction mechanisms in the troposphere.

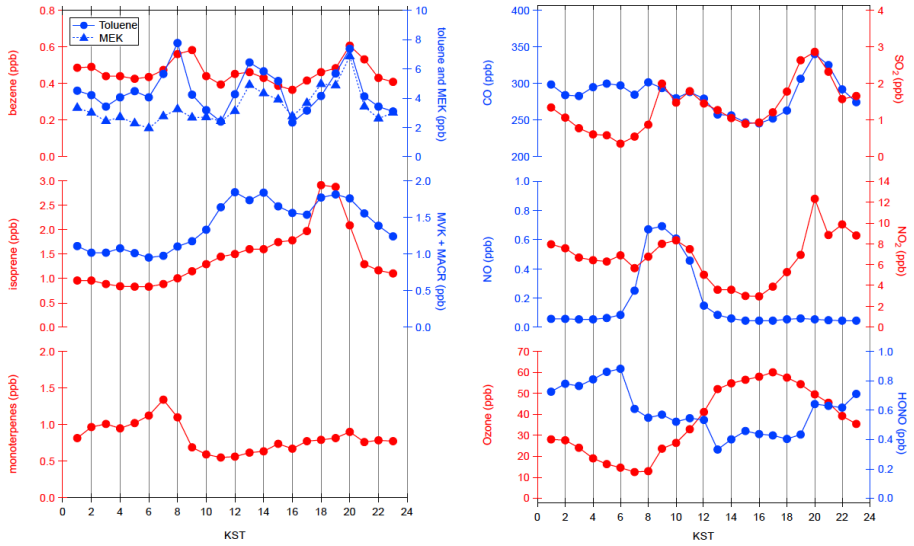

Figure 2. Averaged temporal variations observed trace gases at TRF (1 to 6 June 2012).

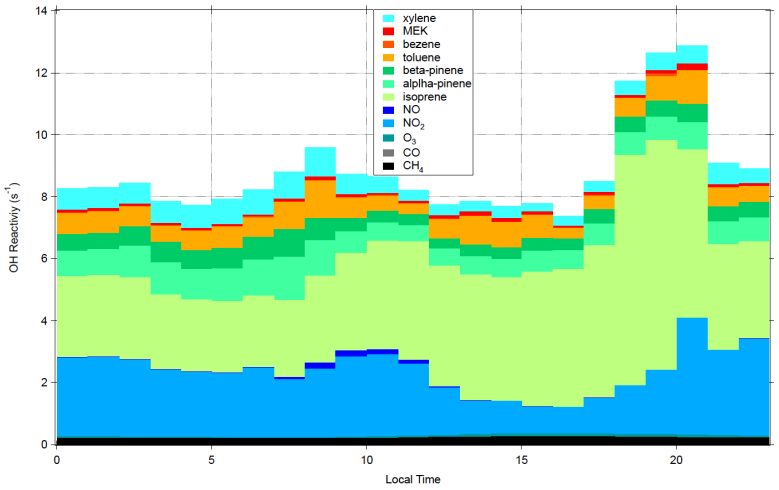

Figure 3. The temporal variations of OH reactivity calculated from the observed dataset at TRF (Fig. 2).

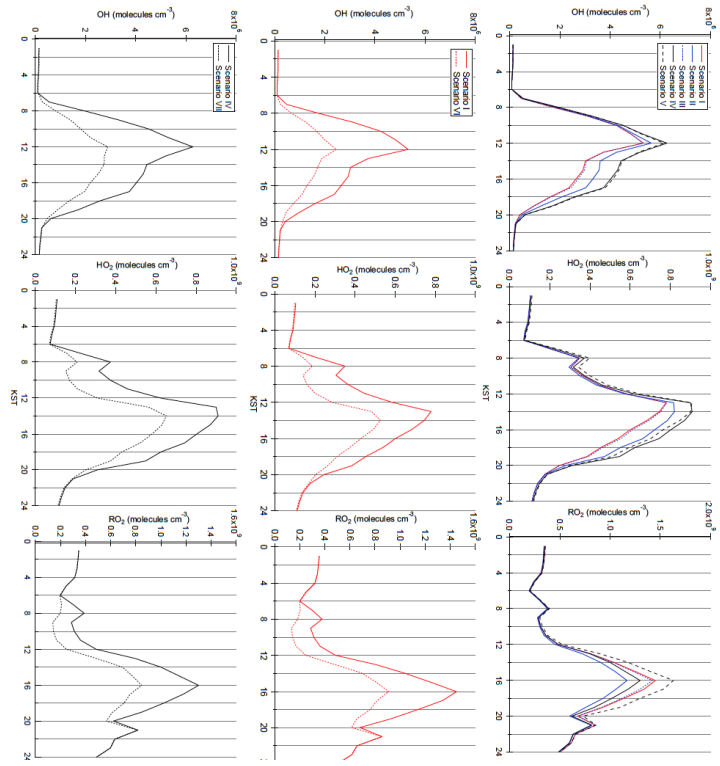

Figure 4. The temporal variations of OH, HO_2, and RO_2 calculated by seven different observationally constrained UWCM box model scenarios.

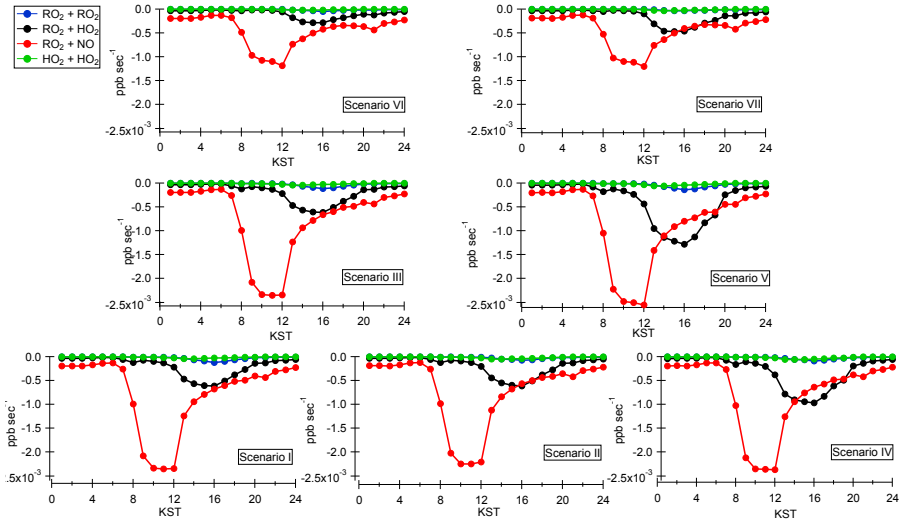

Figure 5. The temporal variations of radical recycling (red) and destruction (blue, black and green) rates calculated using the UWCM box model for different model scenarios.

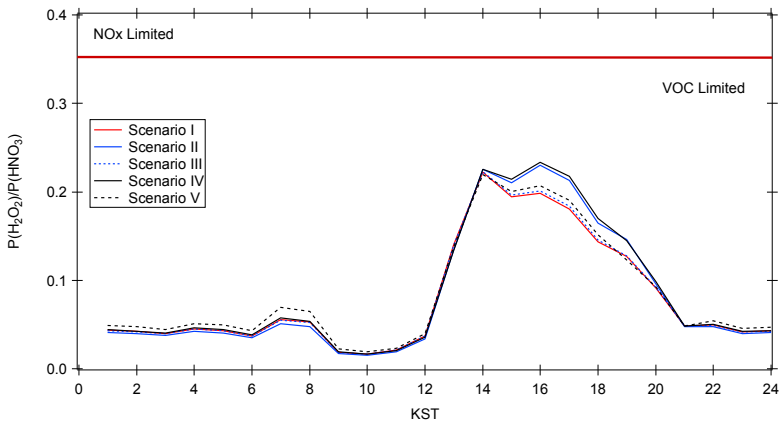

Figure 6. The temporal variations of $P_{H_2O_2}/P_{HNO_3}$ calculated from the UWCM box model from five different model scenarios.

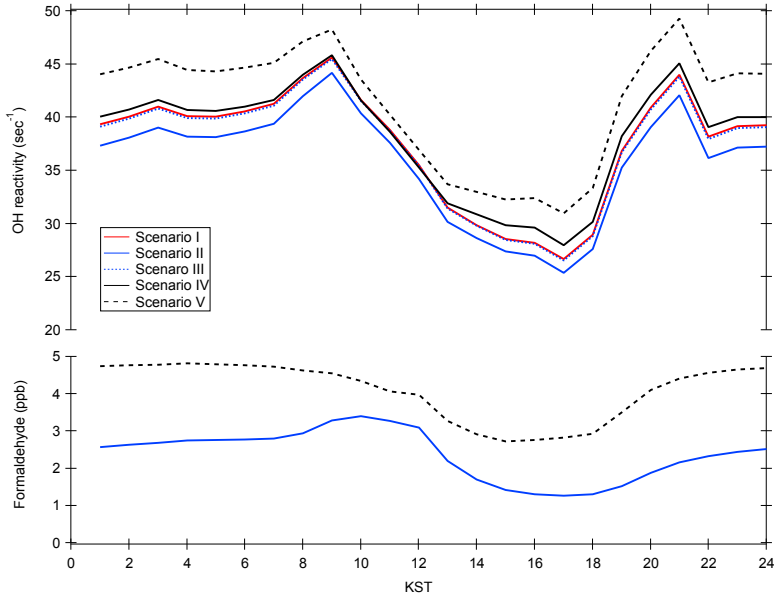

Figure 7. The temporal distributions of UWCM calculated OH reactivity (top panel) and formaldehyde (bottom panel).